



HAL
open science

Determining avalanche modelling input parameters using terrestrial laser scanning technology

A. Prokop, P. Schön, F. Singer, G. Pulfer, Mohamed Naaim, Emmanuel
Thibert

► To cite this version:

A. Prokop, P. Schön, F. Singer, G. Pulfer, Mohamed Naaim, et al.. Determining avalanche modelling input parameters using terrestrial laser scanning technology. International Snow Science Workshop (ISSW), Oct 2013, Grenoble – Chamonix Mont-Blanc, France. p. 770 - p. 774. hal-00950086

HAL Id: hal-00950086

<https://hal.science/hal-00950086>

Submitted on 20 Feb 2014

HAL is a multi-disciplinary open access archive for the deposit and dissemination of scientific research documents, whether they are published or not. The documents may come from teaching and research institutions in France or abroad, or from public or private research centers.

L'archive ouverte pluridisciplinaire **HAL**, est destinée au dépôt et à la diffusion de documents scientifiques de niveau recherche, publiés ou non, émanant des établissements d'enseignement et de recherche français ou étrangers, des laboratoires publics ou privés.

Determining Avalanche Modelling Input Parameters using Terrestrial Laser Scanning Technology

Alexander Prokop¹, Peter Schön¹, Florian Singer¹, Gaëtan Pulfer², Mohamet Naaim² and Emmanuel Thibert²

¹ Institute of Mountain Risk Engineering, Department of Civil Engineering and Natural Hazards, BOKU, University, Vienna, AUSTRIA

² IRSTEA, UR ETGR, Erosion Torentielle Neige et Avalanche, Grenoble France

ABSTRACT: In dynamic avalanche modelling, data about the volumes and areas of the snow released, mobilized and deposited are key input parameters, as well as the fracture height. The fracture height can sometimes be measured in the field, but it is often difficult to access the starting zone due to difficult or dangerous terrain and avalanche hazards. More complex is determining the areas and volumes of snow involved in an avalanche. Such calculations require high-resolution spatial snow surface data from before and after the avalanche. In snow and avalanche research, terrestrial laser scanners are used increasingly to accurately map snow depths over an area of several km². We present data from a terrestrial laser scan campaign of an artificially triggered avalanche at the Col du Lautaret test site (2058 m) in the French Alps and provide data for the validation of dynamic avalanche models. Two terrestrial laser scans from before and after the avalanche release provide the snow surface data required for our analysis. The scans are accurately referenced with surveyed control points and multi-station adjustment, and the resulting data analyzed in GIS. We show the areas and volumes of a) snow released in the starting zones, b) entrained in the track, and c) of the avalanche deposit. Furthermore, we present results for the fracture height, path length, and the track width of the avalanche. Additional measurements from a total station and of snow densities provide the data for comparison and validation of the TLS data. Our results show the ability of TLS to determine avalanche modelling input parameters efficiently and accurately.

KEYWORDS: laser scanning dynamic avalanche modelling modeling

1 INTRODUCTION

In snow and avalanche research, terrestrial laser scanning (TLS) is used increasingly to accurately map snow depths over an area of several km². Laser scanners emit a pulse of light in the near-infrared spectrum. The pulse hits the terrain or snow surface and is reflected. A photodiode in the scanner detects the returning pulse, and determines the distance to the target from the travel time of the pulse. The data from the reflected pulses are saved in a point cloud in the scanner's internal coordinate system. When the exact global position of the laser scanner is known, and three translational and three rotational parameters exist, the point cloud can be registered in a global coordinate system (Prokop, 2008). Prokop (2008), Prokop et al. (2008), and Grünwald et al. (2010) report mean deviations between TLS data and reference tachy-

metry measurements of 0.04-0.1 m for target distances reaching 500 m, depending on the conditions and the laser used.

In dynamic avalanche modelling, release zone area, fracture height, the volumes of snow released in the starting zone and the volumes deposited are key input parameters (Gruber and Bartelt, 2007; Sovilla et al., 2007), as well as data about snow entrainment and deposition in the avalanche path (Eglit and Demidov, 2005; Sovilla and Bartelt, 2002; Sovilla et al., 2007). The height of the crown can often be measured in the field, but the avalanche release zone may be difficult or impossible to access, or continued avalanche hazard prevents a safe investigation. More complex is determining the total volume of snow released, mobilized and deposited in an avalanche. This task requires the application of remote sensing to obtain high-resolution spatial snow surface data from before and after the avalanche. Terrestrial laser scanners can provide a solution for this task.

Corresponding author address: Alexander Prokop, Institute of Mountain Risk Engineering, Institute of Mountain Risk Engineering, Vienna, Austria.
tel: +43 1 47654 4357; fax: +43 1 47654 4390;
email: alexander.prokop@boku.ac.at

2 STUDY SITE

Since several decades, avalanche test sites are used for avalanche dynamics studies. Our research took place at the Col du Lautaret test site, located next to a 2058 m high pass road in

the Hautes-Alpes department in the French Alps. The site is owned and operated by the ETGR (Erosion Torrentielle, Neige et Avalanches) research unit of IRSTEA (Institut national de Recherche en Sciences et Technologies pour l'Environnement et l'Agriculture, previously Cemagref; IRSTEA, 2013). The site comprises a total of eight avalanche paths. Two of these paths are currently equipped with instruments for avalanche research. Measured are avalanche impact pressures, velocities and flow heights (Barbolini and Issler, 2006; Thibert et al., 2008). Informations about the snow conditions are obtained performing manual snow-pits close to the release zone. This includes snow density, temperature, hardness as well as grain types and characteristic size. The data we present is from path n°2 located on the south-east face of the Crête de Chaillol (2600 m). The avalanche path has a length of 800 m, a vertical drop of 450 m, and an average inclination of 34° (Barbolini and Issler, 2006). The avalanches on this path are artificially released with a Gazex remote device (Interfab, 2013).

3 LASER SCANNING AND DATA PROCESSING

In order to detect changes in the snow surface resulting from the avalanche, we had to take two successive scans of the avalanche path, prior and after the avalanche, using a Riegl LPM-321 laser scanner (Figure 1). The best horizontal resolution of the point cloud was 5 cm in a distance of 100 m to the scan position (25 cm in a distance of 500 m).

In order to compare the two scans, we had to align the scans to each other. For the alignment, we applied an iterative closest point (ICP) algorithm available in RiPROFILE, called "multi station adjustment" (Besl and McKay, 1992). This algorithm works best with plane surfaces (Prokop and Panholzer, 2009); in our case, the snow surface provided suited plane surfaces in several places. During the multi-station adjustment, the scan positions were modified iteratively to find a best fit, using tie-points and plane patches placed on both snow surfaces. Additionally, surveyed targets on the slope served as tie-points for the global registration of the scans.

We additionally obtained a topographic survey of the deposit area using a total station (TS Leica TS02) with nearly 30 points. For the distance measurements we used a prism as reflector, which insured a positioning error within a few centimetres, as the station was set 500-700 m of the measured points. A mean horizontal orientation was obtained from 5 control points to get coordinates in the French national grid Lambert zone III (conic conform Lambert projection

from Clarke ellipsoid). In practice, some uncertainty comes from the avalanche deposit edge, which is chosen in the field among snow blocks and aggregates that form in the deposit area due to snow cohesion. The edge of the deposit is then rather positioned with 10-20 cm. Figure 2 plots the avalanche deposit obtained from the TS.



Figure 1. Laser scanner and avalanche.

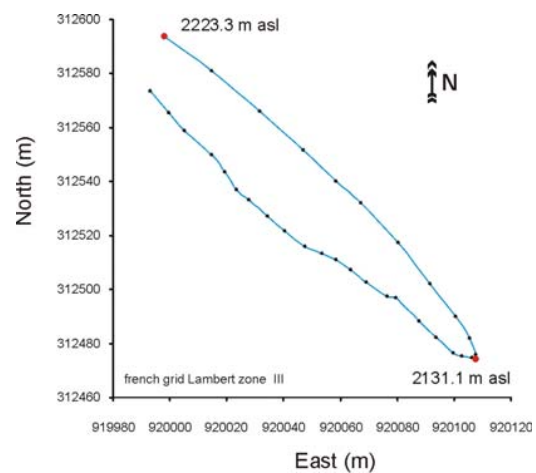


Figure 2. Map of the avalanche deposit as measured from the total station.

The heterogeneously distributed point cloud had to be converted into a raster surface, applying natural neighbor interpolation (Prokop and Panholzer, 2009). In the resulting raster digital snow surface models (DSM), we delineated starting, track and deposit zones. The starting zone we defined as the area where the snow failed, delimited by a fracture line, and the

deposit zone as the zone of avalanche deceleration and debris deposition. As avalanche track we refer to as the zone of avalanche movement and snow mobilization between the starting and deposit zones.

4 RESULTS AND DISCUSSIONS

The avalanche was released around 12h00. At this time, air temperature was still about -10°C . On average, it was a 0.25 m thick layer of fragmented and decomposing particles that released in the avalanche path. There were two starting zones: the upper one (n°1) is a group of 4 small areas, as captured by a time lapse camera (Figure 3), and the second one is located 60-70 m lower in the avalanche track (Figure 4).

The mean snow density in the starting zone was 250 kg/m^3 , ranging from 220 kg/m^3 at the surface to 270 kg/m^3 at the bottom. In the released layer, the particle size was less than 0.5 mm. The snow temperature was between -4.7 and -5°C . Hardness was fist (hand index) and measured as 20 N in Ram Resistance Equivalents. The wetness code is 1 (no water content) for this cold-dry snow layer. At the bottom of the failed slab was a thin 5 cm thick layer containing ice forms, melt forms, and melt-freeze aggregates of about 1 mm. This layer acted as the failure plane. The underlying layers remained stable: At the failure plane interface there was a $\approx 1\text{ cm}$ thick ice crust, and just underneath a layer of rounded grains, less than 0.5 mm in size and 390 kg/m^3 in density.

We analyzed areas and volumes involved in the avalanche in GIS, summarized in Table 1. The two starting zones (Figures 4) had a combined volume of approximately 125 m^3 (Table 1). As displayed in Figure 3, the first starting zone was a complex group of 4 adjoining release areas. This resulted initially in 4 distinct flows, which merged after a few seconds in the main avalanche track to form a single avalanche flow. The release of the slab in the second starting area occurred a few seconds later. The avalanche reached a maximal velocity of 23 m/s at the end of the track at the entrance of the deposition area (Pulfer et al., 2013).

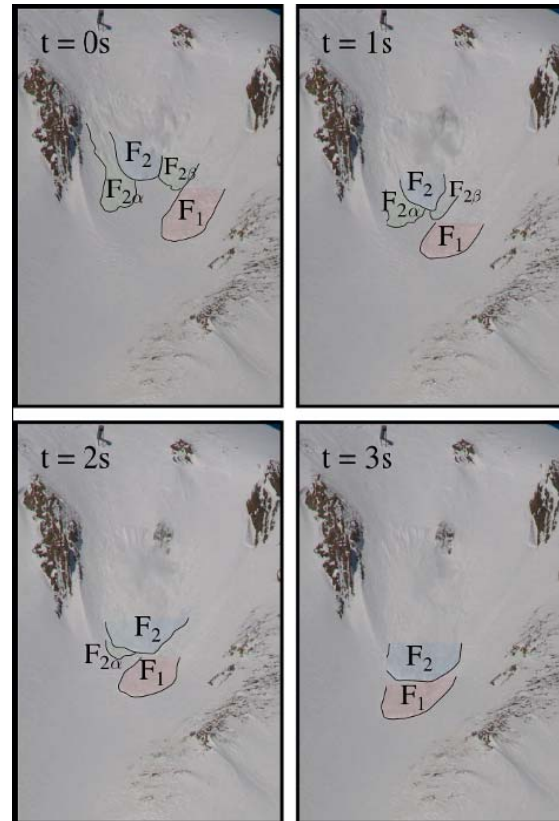


Figure 3. Initial avalanche conditions in the upper starting zone n°1, with 4 release zones initiating 4 flows, which merged after a few seconds. Starting zone n°2 is located in the bottom left corner of the images and the snow there has not yet released.

Snow entrainment refers to the erosion and mobilization of snow in the avalanche track and a subsequent increase in mass of the deposit snow compared to the released snow (Eglit and Demidov, 2005; Sovilla and Bartelt, 2002; Sovilla et al., 2007). In the track zone of our test avalanche, snow entrainment amounts to 300 m^3 . In the run-out zone of the avalanche, about 195 m^3 of snow were deposited (Table 1).

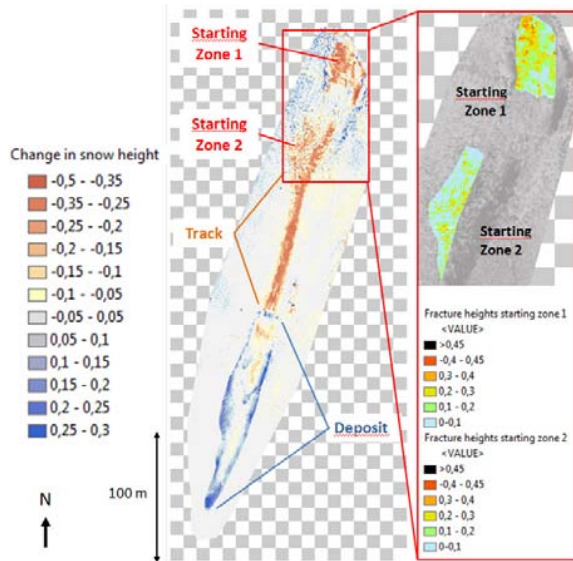


Figure 4. View of the avalanche with the zones and changes in snow height (in meters), and a closer view of the fracture heights (in meters) of the two starting zones; for scale, a 10 m grid is shown.

The avalanche was relatively small and a distinct avalanche crown was absent. We can, however, estimate from our data that the fracture height in the first start zone reached 0.4 - 0.45 m and 0.3 - 0.4 m in the second starting zone (Figure 4; Table 1).

From our measurements with the total station (Figure 2), the deposit area was 157 m in length and had a maximum width of 27 m. These numbers are in agreement with the measured TLS data. Also the volumes of the deposit match quite well. The horizontally projected area obtained from the total station is 2900 m², and the TLS data yields 3000 m² (Table 1).

Table 1. Measured avalanche parameters, obtained with TLS.

Starting volumes (both zones; V_s):	125 m ³
Volume deposited in run-out (V_d)	195 m ³
Ratio $V_d : V_s$:	1.6 : 1
Volume entrained in track (V_{ent}):	300 m ³
Ratio (V_d) : ($V_s + V_{ent}$) :	1 : 2.2
Area of starting zone 1:	500 m ²
Area of starting zone 2:	495 m ²
Area of track zone:	2650 m ²
Area of deposit (in run-out):	3000 m ²
Fracture height starting zone 1:	0.4 – 0.5 m
Fracture height starting zone 2:	0.2 – 0.3 m
Path length:	370m
Width of track (middle):	11 m
Maximum width of deposit:	26 m
Length of deposit:	157 m

The combined volume of snow released in the starting zones and snow entrained in the track zone is higher compared to the volume of deposit snow. This difference in volume can be attributed to a) a densification of snow upon deposition and b) snow cover entrainment along the avalanche path. In the deposit area, we measured a mean density of 380 kg/m³, and in the starting zone of 250 kg/m³, which implies a densification ratio of 1.52 for this avalanche. This is not a high ratio, but the initial snow density was relatively high. McClung and Schaerer (2006) note that deposit snow may be twice as dense as snow in the starting zone, and Sovilla (2004) found during her observations at the Italian test site Pizzac and the Swiss site Vallée de la Sionne ratios of densities between release snow and deposit snow of 1:2 to 1:3.

In our study, the snow released in the starting zones has a combined volume of 125 m³ and the snow deposited 195 m³. An additional volume of 300 m³ was entrained in the track zone, however, resulting in a volume ratio of released and entrained to deposited snow of 1:2.2.

Sovilla (2004) introduced a growth index I_g , defined as:

$$I_g = \frac{M_d}{M_r}, \quad (1)$$

where M_d is the deposit mass, and M_r is the release mass. Using mean snow densities of 250 kg/m³ for the starting zones and 380 kg/m³ for the deposit, M_d is 74100 kg and M_r 31250 kg, resulting in a growth index of 2.4 for this avalanche. Sovilla (2004) observed I_g ratios in her studies at the Pizzac test site of 1.8 - 8.8. Despite the differences in the specific site and avalanche characteristics, her and our results show that a significant amount of snow can be entrained in the avalanche path, even in relatively small avalanche like the one we surveyed at the Col du Lautaret.

5 CONCLUSIONS

We surveyed an artificially triggered avalanche at the Col du Lautaret test site with a terrestrial laser scanner (TLS) and retrieved avalanche parameters required for dynamic avalanche modeling. The data provides information about the areas and volumes of snow released in the starting zone as well as fracture heights, the amount of snow entrained within the avalanche track, and finally the volume of snow deposited. We identified two starting zones, and could determine a volume-ratio between deposited snow on the one, and released and entrained snow on the one hand, of 1:2.2, which

we attribute to the densification of snow during deposition and entrainment in the avalanche track. The growth index of the avalanche is 2.4. The TLS data for length, width of the avalanche and area of the deposit match those obtained by a total station, and the resulting density and volume ratios correspond to density measurements obtained in the field.

The data can be used for the validation of dynamic avalanche models. The different behavior of avalanches due to different topography and snow properties makes such surveys essential for model evaluation.

Our results also underline the ability of TLS to accurately map snow surfaces, supporting the observations from several other studies in the past. Not only are the data accurate, but can be obtained without the difficulties and dangers often associated with field measurements in avalanche zones.

6 ACKNOWLEDGMENTS

The authors wish to thank Xavier Ravanat, Hervé Bellot, Frédéric Ousset and all those who contributed to measurements during the avalanche release operation. Special thanks are due to M. Dumont and C. Carmagnola for their contribution to the snow characterization. We thank Alpinfra (Manfred Scheikl) for providing the laser scanner for this study.

7 REFERENCES

- Barbolini, M. and Issler, D. (Eds.), 2006. Avalanche test sites and research equipment in Europe: an updated overview. Final Report Deliverable D8, SATSIE Avalanche Studies and Model Validation in Europe, 172 pp.
- Besl, P.J. and McKay, N.D., 1992. A method for registration of 3-d shapes, *IEEE Trans. Pat. Anal. and Mach. Intel.*, 14(2), pp. 239–256.
- Eglit, M.E. and Demidov, K.S., 2005: Mathematical modelling of snow entrainment in avalanche motion, *Cold Regions Sci. Tech.* 43, pp. 10-23,.
- Gruber, U. and Bartelt, P., 2007. Snow avalanche hazard modelling of large areas using shallow water numerical methods and GIS, *Environ. Modell. Softw.*, 22, pp. 1472-1481.
- Grünewald, T., Schirmer, M., Mott R., and Lehning, M., 2010. Spatial and temporal variability of snow depth and ablation rates in a small mountain catchment, *The Cryosphere*, 4, pp. 215-225.
- Interfab: Gazex: Lawinenauslösung ohne Sprengstoff. Online:
<http://www.interfab.at/de/Produkte/gazex.html?o=7&parent=LAWINENAUSL%D6SUNG&op=24> (accessed 11 July 2013).
- IRSTEA: Col du Lautaret experimental site. Online:
<http://www.irstea.fr/en/research/research-units/etgr/col-du-lautaret-experimental-site> (accessed 11 July 2013).
- McClung, D.M. and Schaerer, P.A., 2006. *The Avalanche Handbook*, third edition, The Mountaineers Books, Seattle, USA, 342 pp.
- Naaim, M., Taillandier, J.-M., Bouchet, A., Ousset, F., Naaim-Bouvet, F., and Bellot, H., 2001. French avalanche research: experimental test sites, *Extraits de Snow and Avalanches Test Sites / Proceedings of the International Seminar on Snow and Avalanches Test Sites*, Grenoble, 22-23 November 2001, pp. 139-171.
- Prokop, A., 2008. Assessing the applicability of terrestrial laser scanning for spatial snow depth measurements, *Cold Regions Sci. Tech.*, 54, pp. 155–163.
- Prokop, A. and Panholzer, H., 2009. Assessing the capability of terrestrial laser scanning for monitoring slow moving landslides, *Nat. Hazards Earth Syst. Sci.*, 9, pp. 1921–1928.
- Prokop, A., Schirmer, M., Rub, M., Lehning, M., and Stocker, M., 2008. A comparison of measurement methods: Terrestrial laser scanning, tachymetry and snow probing for the determination of spatial snow depth distribution on slopes, *Ann. Glaciol.*, 49, pp. 210-216.
- Pulfer G., Naaim, M., Thibert, E. and A. Soruco, A., 2013, Retrieving avalanche basal friction law from high rate positioning of avalanches. In: *Proceedings ISSW 2013, International Snow Science Workshop 2013, Grenoble-Chamonix*, 6-11, October 2013 (This issue).
- Sovilla, B. and Bartelt, P., 2002. Observations and modelling of snow avalanche entrainment. *Nat. Hazards Earth Syst. Sci.*, 2, 169–179.
- Sovilla, B., 2004. Field experiments and numerical modelling of mass entrainment and deposition processes in snow avalanches, Ph.D. thesis, Swiss Federal Institute of Technology (ETH), Zurich, Switzerland, 191 pp.
- Sovilla, B., Stefan Margreth, S., and Bartel, P., 2007. On snow entrainment in avalanche dynamics calculations, *Cold Regions Sci. Tech.*, 47, pp. 69–79.
- Thibert, E., Baroudi, D., Limam, A., and Berthet-Rambaud, P., 2008. Avalanche impact pressure on an instrumented structure, *Cold Regions Sci. Tech.*, 54, pp. 206-215.